



This discussion paper is/has been under review for the journal Hydrology and Earth System Sciences (HESS). Please refer to the corresponding final paper in HESS if available.

Combining high-resolution satellite images and altimetry to estimate the volume of small lakes

F. Baup¹, F. Frappart^{2,3,4}, and J. Maubant^{1,2,5}

¹Centre d'Études de la BIOSphère (CESBIO), UMR5126, IRD – CNES – OMP – INSU – Université de Toulouse, 24 rue d'Embaquès, 32000 Auch, France

²Géosciences Environnement Toulouse (GET), Observatoire de Midi-Pyrénées, Université de Toulouse, CNRS, IRD, 14 avenue Edouard Belin, 31400 Toulouse, France

³Laboratoire d'Etudes en Géophysique et Océanographie Spatiales (LEGOS), UMR5566, Observatoire de Midi-Pyrénées, Université de Toulouse, CNES, CNRS, IRD, 14 avenue Edouard Belin, 31400 Toulouse, France

⁴Groupe de Recherche en Géodésie Spatiale (GRGS), France

⁵École Supérieure des Géomètres et Topographes (ESGT), 1 boulevard Pythagore, 72 000 le Mans, France

Title Page

Abstract

Introduction

Conclusions

References

Tables

Figures



Back

Close

Full Screen / Esc

Printer-friendly Version

Interactive Discussion



Received: 18 November 2013 – Accepted: 29 November 2013

– Published: 20 December 2013

Correspondence to: F. Baup (frederic.baup@cesbio.cnes.fr)

Published by Copernicus Publications on behalf of the European Geosciences Union.

HESSD

10, 15731–15770, 2013

Volume of small lakes

F. Baup et al.

Title Page

Abstract

Introduction

Conclusions

References

Tables

Figures



Back

Close

Full Screen / Esc

Printer-friendly Version

Interactive Discussion



Abstract

This study presents an approach to determine the volume of water in small lakes (< 100 ha) by combining satellite altimetry data and high-resolution (HR) images. The lake being studied is located in the south-west of France and is only used for agricultural irrigation purposes. The altimetry satellite data are provided by RA-2 sensor on board Envisat, and the high-resolution images (< 10 m) are obtained from optical (Formosat-2) and synthetic aperture radar (SAR) sensors (Terrasar-X and Radarsat-2) satellites. The altimetry data (data are obtained every 35 days) and the HR images (45) have been available since 2003 and 2010, respectively. In situ data (for the water levels and volumes) going back to 2003 have been provided by the manager of the lake. Three independent approaches are developed to estimate the lake volume and its temporal variability. The first two approaches are empirical and use synchronous ground measurements of the water volume and the satellite data. The results demonstrate that altimetry and imagery can be effectively and accurately used to monitor the temporal variations of the lake ($R^2_{\text{altimetry}} = 0.97$, $\text{RMSE}_{\text{altimetry}} = 5.2\%$, $R^2_{\text{imagery}} = 0.90$, and $\text{RMSE}_{\text{imagery}} = 7.4\%$). The third method combines altimetry (to measure the lake level) and satellite images (of the lake surface) to estimate the volume changes of the lake and produces the best results ($R^2 = 0.99$) of the three methods, demonstrating the potential of future Sentinel and SWOT missions to monitor small lakes and reservoirs for agricultural and irrigation applications.

1 Introduction

Water supply issues are creating unprecedented pressures because of increasing population and economic demands. As irrigated agriculture represents 70 % of global water consumption, managing water resources is a major concern in maintaining sustainable agricultural practices. Water management will become even more relevant in the future as urbanisation, industrialisation, and climate change exert greater pressures on water

HESSD

10, 15731–15770, 2013

Volume of small lakes

F. Baup et al.

Title Page

Abstract

Introduction

Conclusions

References

Tables

Figures

⏪

⏩

◀

▶

Back

Close

Full Screen / Esc

Printer-friendly Version

Interactive Discussion



[Title Page](#)[Abstract](#)[Introduction](#)[Conclusions](#)[References](#)[Tables](#)[Figures](#)[⏪](#)[⏩](#)[◀](#)[▶](#)[Back](#)[Close](#)[Full Screen / Esc](#)[Printer-friendly Version](#)[Interactive Discussion](#)

use (OECD, 2012). Water resources can be monitored at a global scale using three approaches: in situ measurements, modelling, and remote sensing observations (Jorgensen et al., 2005; Harding et al., 2011; Hall et al., 2011; Duan and Bastiaanssen, 2013). Given the dramatic decrease in the number of in situ gauges available in recent years and the difficulty of modelling water resources at a global scale (because of complex mixing between inflows and outflows), measuring water stages by remote sensing and especially by satellite has become a major goal in hydrology for the coming decades (The Ad Hoc Group on Global Water Datasets, 2001; Alsdorf et al., 2007; Duan and Bastiaanssen, 2013).

Satellite radar altimetry was originally developed to accurately measure ocean surface topography and has been successfully used to obtain valuable information for land hydrology by estimating the variation in lake water levels (Birkett, 1995; Cazenave et al., 1997; Crétaux et al., 2011), rivers (Birkett, 1998; Birkett et al., 2002; Frappart et al., 2006a; Santos da Silva et al., 2010), and floodplains (Frappart et al., 2006b, 2008; Santos da Silva et al., 2012). The accuracy of altimetry-based water levels can vary from 5 to 80 cm depending on the altimetry data used (i.e., from Topex/Poseidon and ERS-2 to Envisat and Jason-2), the size of the water bodies being flown over, the configuration of the terrain, and the presence of vegetation (Frappart et al., 2005, 2006a, b; Santos da Silva et al., 2010; Crétaux et al., 2011; Ricko et al., 2012).

However, comprehensive monitoring of surface resources also requires knowledge of the extent of the surface water and the water volume. Earth observation missions have been developed to provide images of the Earth's surface at various spatial, temporal, and spectral resolutions, which have been used to map land use and land cover dynamics over the last few decades (Kümmerle et al., 2013; Klein et al., 2014). Past, current (ALOS, ENVISAT, Formosat-2, Radarsat-2, Spot 4–5, TerraSAR-X...), and future (Radarsat Constellation, Sentinel 1–2, TerraSAR-L...) Earth observation missions offer high spatial resolution, frequent revisit times, and a unique opportunity to monitor the extent of global water resources, even small-sized resources. Among other applications, high-resolution images were recently used to inventory tank irrigation systems

in India (Abdul Hakeem and Raju, 2009), detect lakes and river courses in various environments (Strozzi et al., 2012; Karbouche and Clavet, 2013), and monitor the spatial distribution and temporal dynamics of wetlands (Zhou et al., 2010; White and Lewis, 2011).

Recent studies have demonstrated the potential of combining satellite imagery and radar altimetry to estimate the volume of water stored in lakes, rivers, and floodplains and how these volumes change in response to climate variability and/or anthropogenic effects using SAR images, multispectral images, or multi-satellite observations (Frappart et al., 2005, 2006b, 2013; Yesou et al., 2007; Ding and Li, 2011; Haibo et al., 2011; Wang et al., 2011; Duan and Bastiaanssen, 2013). Despite the relevance of these results, these techniques have not been applied to the study of small lakes.

In this study, we developed a method to estimate the water volume of small lakes (< 100 ha) by combining satellite altimetry and high-resolution imagery. The method was used to determine the variation in the volume of Lake “la Bure”, a small reservoir (with an average area of 52 ha) located in an irrigated agricultural area in the south-west of France. This study is structured as follows: the primary characteristics of the study site, satellite data, and in situ data are presented in Sect. 1. In Sect. 2, three different methods are presented for estimating the water volume of the lake. The results are analysed and discussed in Sect. 3, in which the HR images, altimetry, and a combination of the two techniques is used to accurately estimate seasonal changes in the water volume. Concluding remarks and future work are presented in Sect. 4.

2 Study area and datasets

2.1 Study area

Lake “la Bure” (43°24′54″ N; 1°09′07″ E) is located in the south-west of France, close to the city of Rieumes (which is 40 km south-west of the city of Toulouse), in a study area monitored by CESBIO in the framework of the “Sud-Ouest” Project (Dejoux et al.,

Title Page

Abstract

Introduction

Conclusions

References

Tables

Figures



Back

Close

Full Screen / Esc

Printer-friendly Version

Interactive Discussion



[Title Page](#)[Abstract](#)[Introduction](#)[Conclusions](#)[References](#)[Tables](#)[Figures](#)[|◀](#)[▶|](#)[◀](#)[▶](#)[Back](#)[Close](#)[Full Screen / Esc](#)[Printer-friendly Version](#)[Interactive Discussion](#)

2012; Baup et al., 2012; Fieuzal et al., 2012, 2013) (Fig. 1). The area has a temperate climate with a mean annual rainfall of approximately 600 mm. Rainfalls are regularly distributed (with a monthly mean of 50 mm), with a maximum of 80 mm in the spring and a minimum of 32 mm in the summer according to the records from meteorological station number 3145400 of Météo-France, the French Meteorological agency (<http://www.meteofrance.fr>). Inside the watershed (20.70 km²) of the lake, the relief is not clearly delineated (min = 0 %, max = 16.9 %, and mean slope = 2.8 %), and the land use is composed of crops (40.90 %), forest (24.02 %), grassland (33.4 %), and water bodies (1.68 %). Lake “la Bure” is an artificial reservoir that was constructed in 1987 for crop irrigation purposes. Since its construction, the barrage has been managed by the SIAH (Syndicat Intercommunal d’Aménagement Hydraulique de la vallée du Touch et de ses affluents) company. The extent of the lake can reach 52 ha for a maximum water volume of 4 million m³. The charge and discharge of the lake only occur via rainfall events (throughout the year) and irrigation pumping (primarily in the summer). The lake is located under Envisat RA-2 altimetry track 773 and is inside the footprint of three high-resolution images that are acquired by the Formosat-2, TerraSAR-X, and Radarsat-2 satellites.

2.2 Satellite data

The satellite data used in this study were composed of HR images and altimetry data. Forty-five HR images were acquired in 2010, between January and November, by sensors on board three different low-orbiting satellites (Radarsat-2, TerraSAR-X, and Formosat-2) (Fig. 2). Thirty-three of these images were acquired in the microwave domain using SAR instruments (Radarsat-2 and TerraSAR-X), and 12 were acquired using the multispectral mode of the Formosat-2 satellite. The altimetry data were acquired by the Envisat RA-2 sensor between February 2002 and October 2010.

2.2.1 SAR images

The SAR images were acquired at X- and C-bands by TERRASAR-X and RADARSAT-2, respectively (Table 1).

TerraSAR-X is a German Earth observation satellite that was launched in June 2007 (Fritz et al., 2008; Breit et al., 2010). The SAR instrument on board the satellite operates in the X-band ($f = 9.65$ GHz and $\lambda = 3.1$ cm). All of the images (which numbered 18 in 2010) were provided by the German Aerospace Centre (DLR) and were acquired with the same polarisation state (HH) for incidence angles ranging from 27.3° to 53.3° to increase the repetitiveness of observations from an initial 11 day orbital cycle. Two acquisition modes were combined: StripMap (SM) and SpotLight (SL), which were characterised by pixel spacings of approximately 3 and 1.5 m, respectively. The backscattering coefficients were calculated using Eq. (1) (Lavalle, 2009):

$$\sigma_{pq}^O = 20 \log(DN_{pq}) + 10 \log(CF_{pq}) + 10 \log(\sin(\theta)) \quad (1)$$

where DN denotes the digital number of pixels, CF denotes the calibration factor, and θ denotes the incidence angle. The indexes p and q denote the linear polarisation states of the electromagnetic wave (H or V), respectively.

The Canadian satellite Radarsat-2 was launched in December 2007 (Morena et al., 2004). Its payload encompasses a SAR instrument operating in the C-band ($f = 5.405$ GHz and $\lambda = 5.5$ cm). The orbital cycle of the satellite is 24 days, but different orbit and incidence angles can be combined to increase the numbers of possible acquisitions per cycle. The images (which numbered 15 in 2010) were provided by the Canadian Space Agency through the SOAR (Science and Operational Application Research) program and were all acquired in full quad-polarisation mode (Fine Quad-Pol: HH, VV, HV, and VH). The incidence angles ranged from 23° (FQ5) to 41° (FQ21) with a pixel spacing of 5 m. The images were calibrated using NEST software (NEST, 2013) and Eq. (2) (Skriver et al., 1999):

$$\sigma_i^O = 20 \log_{10}(DN_i/A2_i) + 10 \log_{10}(\sin(\theta_i)) \quad (2)$$

15737

HESSD

10, 15731–15770, 2013

Volume of small lakes

F. Baup et al.

Title Page

Abstract

Introduction

Conclusions

References

Tables

Figures

⏪

⏩

◀

▶

Back

Close

Full Screen / Esc

Printer-friendly Version

Interactive Discussion



where DN_i denotes the digital number of the pixel “ i ”, θ denotes the incidence angle, and $A2$ denotes the gain (which is provided by the image product data table).

All of the SAR images were geo-referenced using aerial IGN ortho-photos (with a spatial resolution of 50 cm). The ortho-photos were first resized to the resolution of the image and then 70 reference points were taken between the base (IGN ortho-photos) and wrap images (satellite data). The geo-location accuracy was under 2 pixels (i.e., 3 to 6 m) on average for the different products. Finally, all of the radar images were filtered to reduce speckle effects using a Gamma filter with a filtering window of 6 by 6 pixels.

2.2.2 Optical images

The optical images (12) were provided by the Taiwanese Formosat-2 satellite (which was launched in 2004) for four narrow wavelengths between 0.45 and 0.90 μm corresponding to the blue, green, red, and near-infrared ranges (Liu, 2006; Chern et al., 2008, Table 1). All of the images used in this study were acquired in multispectral mode (MS) with a theoretical daily orbital cycle (sun-synchronous orbit) at the same viewing angle ($\pm 45^\circ$). This mode was characterised by a spatial resolution of 8 m for a scene coverage of 24 km \times 24 km. All of the images were ortho-rectified using CNES ortho-rectification tools. Cloud detection and atmospheric correction were also applied (Sand et al., 2006; Hagolle et al., 2010).

2.2.3 Altimetry data

RA-2 (Advanced Radar Altimeter) is a nadir-looking pulse-limited radar altimeter on board ENVISAT that operates at two frequencies: the Ku-band (13.575 GHz/wavelength of 2.3 cm) and the S-band (3.2 GHz/9.3 cm) (Zelli, 1999). The Geophysical Data Records (GDRs) distributed by ESA (ESA, 2002) include accurate satellite positions (i.e., the longitude, latitude, and altitude of the satellite in its orbit) and timing; altimeter ranges; instrumental, propagation, and geophysical corrections

Title Page

Abstract

Introduction

Conclusions

References

Tables

Figures

⏪

⏩

◀

▶

Back

Close

Full Screen / Esc

Printer-friendly Version

Interactive Discussion



[Title Page](#)[Abstract](#)[Introduction](#)[Conclusions](#)[References](#)[Tables](#)[Figures](#)[◀](#)[▶](#)[◀](#)[▶](#)[Back](#)[Close](#)[Full Screen / Esc](#)[Printer-friendly Version](#)[Interactive Discussion](#)

applied to the range; and several other parameters used to build altimetry-based water levels. For the ENVISAT mission, four different retracking algorithms are operationally applied to RA-2 raw data to provide range estimates and backscattering coefficients. Each retracking algorithm, namely Ocean, Ice-1, Ice-2, and Sea-Ice, has been developed for a specific type of surface, but none of these algorithms has been specifically designed for processing altimeter echoes over land (Brown, 1977; Wingham et al., 1986; Laxon, 1994; Legrésy and Rémy, 1997). Previous studies have shown that the Ice-1 algorithm measures the water levels of small lakes and reservoirs, rivers, and floodplains most accurately (Frappart et al., 2006a; Santos da Silva et al., 2010; Ricko et al., 2012). In this study, the altimetry measurements contained in the ENVISAT RA-2 GDRs were made available by the Centre de Topographie des Océans et de l'Hydrosphère (CTOH – <http://ctoh.legos.obs-mip.fr/>) for February 2002 to October 2010 (cycles 8 to 93), corresponding to the reference repetitive orbit of the satellite.

2.3 In situ data

The monthly rainfall data came from the records of weather station number 3145400, which is located less than five kilometres from the centre of the lake and is operated by the French meteorology Agency (Météo France). The relationship between the water levels and the volume of water stored in the lake was established in 1987 when the lake was dug (Fig. 3). More recent information on the storage capacity of the lake is available from bathymetric surveys that were performed in 2010 by AEAD (“Agence de l’Eau Adour-Garonne”, which depends of the Ministry of Ecology, Sustainable Development, and Energy). The water levels were recorded at two different time steps, pressure probes were used to obtain automatic weekly measurements, and monthly data were provided by gauge readings. Figure 4 shows the temporal variations in the volume of water stored in Lake “la Bure” over the study period. The difference between the volume obtained from the in situ water levels and the volume obtained from the bathymetric survey performed in 2010 was less than 2%. This difference was attributed both

to the accuracy of the bathymetric measurements and to possible siltation. Various characteristics of the available ground data are summarised in Table 2.

3 Methodology

Figure 5 summarises the methods used to monitor the water volume of Lake “la Bure”. The satellite data acquired within the optical and microwave domains were processed to estimate the water surfaces (using HR images) and levels (using altimetry) throughout the hydrological cycle. The temporal variations in the volume storage of the lake was finally estimated by combining one type of satellite data (HR images or radar altimetry) with ground measurements or using two types of complementary satellite data.

3.1 Determination of the extent of the lake area from satellite imagery

An automatic parallelepiped classification was performed using ENVI software on each HR image to determine which pixels could be associated with open water (Richards, 1999; ENVI, 2004; Lillesand et al., 2008). This supervised classification method relied on a simple logical rule to classify a given pixel based on its radiometry (4 channels are considered: blue, green, red, and near infra-red). The decision boundaries formed a 4-dimensional parallelepiped in the image data space. Each class was defined in terms of a threshold for the standard deviation from the mean of each training site (i.e., the region of interest). Four classes were identified as being representative of the landscape: forests, open water, bare soils, and crops. Once the classification process was completed, all of the surface elements that were identified as open water were vectorised and exported to an ArcGIS shape file format in which the boundary represents the lake shoreline (artefacts in the polygon that represented open water were suppressed using the FillHoles toolbox of the software). Figure 6 shows the temporal variations in the lake shoreline for four different dates in 2010 that were acquired by the Radarsat-2 satellite.

[Title Page](#)

[Abstract](#)

[Introduction](#)

[Conclusions](#)

[References](#)

[Tables](#)

[Figures](#)



[Back](#)

[Close](#)

[Full Screen / Esc](#)

[Printer-friendly Version](#)

[Interactive Discussion](#)



3.2 Altimetry-based water levels

The principle behind radar altimetry is as follows: the altimeter emits a radar pulse and measures the two-way travel-time from the satellite to the surface. The distance between the satellite and the Earth surface – the altimeter range (R) – is thus derived with a precision of a few centimetres. The satellite altitude (H) with reference to an ellipsoid is also accurately known from orbitography modelling. Taking into account propagation delays from the interactions of electromagnetic waves in the atmosphere and geophysical corrections, the height of the reflecting surface (h) with reference to an ellipsoid or a geoid can be estimated as follows:

$$h = H - R - C_{\text{ionosphere}} - C_{\text{dry troposphere}} - C_{\text{wet troposphere}} - C_{\text{solid Earth tide}} - C_{\text{pole tide}} \quad (3)$$

where $C_{\text{ionosphere}}$ is the correction for delayed propagation through the ionosphere, $C_{\text{dry troposphere}}$ and $C_{\text{wet troposphere}}$ are corrections for delayed propagation in the troposphere from pressure and humidity variations, respectively, and $C_{\text{solid Earth tide}}$ and $C_{\text{polar tide}}$ are corrections that account for crustal vertical motions from the solid and polar tides, respectively.

An altimetry station, which is the equivalent of an in situ water level gauge, can be defined at each intersection between a lake, a river, or a floodplain and the satellite ground-track. For each altimeter pass or cycle, the altimetry measurements are processed using the three following primary steps to obtain a water level: a 2-D selection is made from the data contained in the window corresponding to the altimetry station using satellite imagery; the altimetry heights from Eq. (3) are filtered (at varying degrees of complexity depending on the approach chosen) using a statistical and/or hydrological criterion; and the altimetry-based water level is computed using estimates of either the median or the mean of the selected altimetry heights, which may or may not have been corrected for hooking effects (Frappart et al., 2006a; Santos da Silva et al., 2010). This process is repeated for each cycle to construct a water level time-series at the altimetry station. In this study, Virtual ALtimetry Station (VALS) software

Title Page

Abstract

Introduction

Conclusions

References

Tables

Figures



Back

Close

Full Screen / Esc

Printer-friendly Version

Interactive Discussion



was used to derive the time-series of water levels for Lake “la Bure” from ENVISAT RA-2 data from February 2002 to October 2010. The processing of altimetry data using VALS consisted of three primary steps:

1. a coarse selection of the altimetry data over the water body contained in a polyline using Google Earth was obtained,
2. the VALS visualisation tool was used to obtain a refined selection of the valid altimetry-derived water levels in which outliers were removed and the hooking effects were likely to be corrected for and
3. the time-series of water levels was computed using the median value of all of the valid altimetry-based water levels for each cycle.

Further details on processing the altimetry data using VALS software can be found in Santos da Silva et al., 2010. At the end of the process, 70% of the data remained.

3.3 Lake volume estimates

Three independent approaches were developed to estimate the lake volume and its temporal variability. In the first two methods, an empirical relationship between either the lake surface derived from the HR images or the altimetry-based water levels and quasi-synchronous estimates of the lake volume was determined from the in situ water level measurements. In the third method, the lake surface from the HR images was combined with altimetry-based water levels that were acquired quasi-synchronously to estimate the volume of the lake. A combination of satellite products was used to estimate the change in the lake volume from both the variation in the water level and the surface. To this end, the lake of interest was modelled as a simple geometric shape, for which the variation in the water volume (ΔV) between two dates (t_1 and t_2 , respectively)

Title Page

Abstract

Introduction

Conclusions

References

Tables

Figures



Back

Close

Full Screen / Esc

Printer-friendly Version

Interactive Discussion



was computed using Eqs. 4 and 5:

$$\text{If } \Delta H > 0 \text{ then } \Delta V = S(t_1) \cdot \Delta H + (\Delta H \cdot \Delta S)/2 \quad (4)$$

$$\text{If } \Delta H < 0 \text{ then } \Delta V = -((S(t_1) - |\Delta S|) \cdot \Delta H + (\Delta H \cdot \Delta S)/2) \quad (5)$$

5 where $\Delta H = H(t_2) - H(t_1)$ and $\Delta V = V(t_2) - V(t_1)$ denote the difference in the water levels (H) and the volume between two dates, t_1 and t_2 , respectively. $\Delta S = S(t_2) - S(t_1)$ denotes the variation in the surface between the two dates.

4 Results and discussion

4.1 Estimating the lake volume using HR images

10 Figure 7 shows the temporal evolution of the water surface of Lake “la Bure” for the complete series of 45 HR images that were acquired in 2010. The lake surface was estimated by applying the method presented in Sect. 3.1 to the Formosat-2, Radarsat-2, and TerraSAR-X images that were acquired in 2010. The measurement of the temporal behaviour of the lake surface from the three sensors was highly consistent and
15 ranged between 42 and 52 ha. The difference between the three estimates never exceeded 3.94 ha (for an RRMSE of 8.5 %) and equalled 0.51 ha (which was 1.1 % of the mean water surface) when averaged over the complete period of observation for the quasi-synchronous satellite acquisitions (i.e., time-lags below 5 days).

The annual cycle of the open water surface consists of two phases: the filling of the lake (from the end of September to mid-June) and the emptying of the lake (during the summer). The filling of the lake only occurs through rainfall events (primarily from runoff inside the watershed). The lake surface significantly increases over this period. No additional pumping is needed to fill the lake more rapidly, unlike some of the other lakes in the region studied. The lake empties during the irrigation period, which occurs
20 between July and October (Fig. 7). In the summertime, the low amount of rainfall is not sufficient to compensate for losses from irrigation and evaporation.

[Title Page](#)[Abstract](#)[Introduction](#)[Conclusions](#)[References](#)[Tables](#)[Figures](#)[⏪](#)[⏩](#)[◀](#)[▶](#)[Back](#)[Close](#)[Full Screen / Esc](#)[Printer-friendly Version](#)[Interactive Discussion](#)

Figure 8 shows an empirical relationship between the estimates of the lake surface from the HR images and the volume measurements. The relationship is clearly non-linear (i.e., a 2nd-order polynomial function) with a coefficient of determination of 0.90 and a mean error of $200\,000\text{ m}^3$ for the volume estimates (i.e., 7.4% of the average water volume in 2010). In agreement with the bathymetric measurements, the surface changed dramatically (from 40 to 44 ha) for small volume changes between 2.2 and 2.5 hm^3 when the filling began (sensitivity of $80\,000\text{ m}^3\text{ ha}^{-1}$). The relationship is fairly linear for volume changes from 2.5 hm^3 to greater than 4 hm^3 , with a higher sensitivity compared to the beginning of the filling phase ($237\,000\text{ m}^3\text{ ha}^{-1}$).

4.2 Estimating the lake volume from altimetry

4.2.1 Validation of altimetry-based water levels

The altimetry data (RA-2) were validated by directly comparing the altimetry-based water levels with the in situ water levels from gauge measurements made by the Lake Management Institute (SIAH) over the 2003–2010 period (Fig. 9). Similar temporal variations were observed for both datasets, in which the in situ water levels exhibited annual (peak to peak) amplitudes between 2.65 m (2007/2008) and 5.36 m (2003/2004). Both the seasonal variations (i.e., the maxima from May to June and the minima from September to October) and the inter-annual variations (i.e., the minimum during the drought of 2003) were also successfully detected. Although the difference between the in situ and altimetry-derived water levels reached 1.3 m one time, it did not exceed 0.3 m in 75% of the cases studied. The RMSE and R^2 were equal to 0.31 m and 0.99, respectively, showing that the two sources of data were in very good agreement. The results obtained in this study were comparable to results for large lakes (Crétau and Birkett, 2006; Ricko et al., 2012; Duan and Bastiaanssen, 2013) and large rivers (Frappart et al., 2006a; Santos da Silva et al., 2010) and were better than those obtained for various small rivers (Santos da Silva et al., 2010).

4.2.2 Pluri-annual water volume estimates

Figure 10 shows the empirical relationship that was obtained between the ground-measured volumes and the altimetry-derived water levels. Sixty-five measurements were used from the period between 2003 and 2010 to obtain a 3rd-order polynomial that related the altimetry-based water levels to the water volume stored in the lake. The statistical parameters highlighted the quality of the regression ($R^2 = 0.97$, RMSE = 0.14 hm³, and RRMSE = 5.3%). No yearly dependence was observed, confirming the temporal stability of the method.

For subsequent comparison with the HR images, a specific empirical relationship relating altimetry-based water levels to water volumes was determined for 2010 (Sect. 4.3). Figure 11 compares the water volumes that were estimated using these two relationships. The results were very similar, although the results obtained using the empirical function that was determined using over 8 yr of altimetry data were slightly more accurate than those obtained using the empirical function for 2010 (Table 3). The lake volume estimates never exceeded 0.17 hm³ and corresponded to a high coefficient of determination ($R^2 \geq 0.96$) and a low relative error (i.e., the mean lake volume had an RRMSE of 6.4%).

4.3 Combined use of HR images and altimeter data

In this section, we show how variations in the lake volume were obtained by combining the HR images (Sects. 2.2.1 and 2.2.2.) with the altimetry-derived water levels (Sect. 2.2.3). This approach was validated for 2010, for which satellite images and altimetry data were simultaneously available to compare with in situ measurements of the lake volume. Figure 12 shows the temporal variations in the lake volume that were estimated using three different methods: ground measurements (SIAH), HR images (Sect. 3.1.), and altimetry-based water levels (Sect. 3.2.). In 2010, the emptying and refilling phases of the lake were accurately detected and reproduced by both the satellite estimates. The errors were equal to 0.20 and 0.14 hm³ using the HR images and

HESSD

10, 15731–15770, 2013

Volume of small lakes

F. Baup et al.

Title Page

Abstract

Introduction

Conclusions

References

Tables

Figures

⏪

⏩

◀

▶

Back

Close

Full Screen / Esc

Printer-friendly Version

Interactive Discussion



[Title Page](#)[Abstract](#)[Introduction](#)[Conclusions](#)[References](#)[Tables](#)[Figures](#)[⏪](#)[⏩](#)[◀](#)[▶](#)[Back](#)[Close](#)[Full Screen / Esc](#)[Printer-friendly Version](#)[Interactive Discussion](#)

the RA-2 data, respectively. All of the altimeter-derived volumes had an error below 5 % of the measured volume; whereas only half of the HR-image-based volume estimates reached this level of accuracy. The precision for the estimated lake volume obtained using all of the satellite products was always below 19 %. Figure 13 shows the relationship that was estimated between the water level obtained using the satellite products (from RA-2) and the water surface (from the HR images). Only the satellite acquisitions that were performed quasi-synchronously (for a time-lag below 5 days) were retained to reduce the signal scattering because of the potential variation in the lake properties (i.e., the surface, level, and volume) between the images and the altimeter acquisitions. The two satellite products were strongly linearly correlated with a high coefficient of determination ($R^2 = 0.94$).

Figure 14 shows the relationship that was obtained between the variations in the volume estimated using the ground measurements and the satellite products. Five dates were retained in accordance with the two following constraints:

- the satellite acquisitions were performed in 2010,
- the altimetry data and HR images were acquired for a time lag below 5 days (so implying that ΔV was less than 0.7 % of the average volume during this period using the relationship between the water levels and the water volumes stored in Lake “la Bure”, as shown in Fig. 3).

The ground-based estimates of the variations in the water volume shown in Fig. 14 were in very good agreement with the results from this approach (i.e., $R^2 = 0.98$, RMSE = 0.06 hm^3 , and the linear regression slope was close to 1). The major drawbacks of this method are its low temporal resolution, which depends on the availability of data obtained around the same time period from both satellites, and the fact that only variations in the volume and not the volumes themselves can be determined. Figure 14 also shows the estimates of the variations in the water volume from the RA-2 altimetry-based water levels and the in situ data, and the HR images and the in situ data for the same dates. The two estimates were in very good agreement with the volume

derived from the in situ data ($R^2 = 0.95$ and $RMSE = 0.17 \text{ hm}^3$ for altimetry-based volume variations and $R^2 = 0.90$ and $RMSE = 0.25 \text{ hm}^3$ for the HR-image-based volume variations); however, more accurate results were obtained by estimating the water volumes using altimetry and imagery. These results need to be confirmed for longer time-series. The results confirmed the efficacy of these products to estimate the temporal volume changes of the lake ($R^2 \geq 0.90$). A strong limitation of the last two relationships is that they require in situ data.

5 Conclusion and perspectives

This study demonstrated the high potential of remotely sensed observations (HR images and radar altimetry) for accurately monitoring the surface volume of small lakes and reservoirs (i.e., with areas $< 100 \text{ ha}$). Three different approaches were developed that combined quasi-synchronous multi-satellite data and/or in situ measurements to monitor the temporal variations in water resources. All of these methods provided reliable estimates of the variations in the water volume with an average accuracy greater than 7.4 % of the average volume.

In the first method (Sect. 4.1.), the water surface estimates were converted from multispectral HR images into water volumes using in situ measurements. For our study site, this method enabled the volumes of water stored in the lake on a weekly basis to be monitored continuously. The high correlation ($R^2 = 0.90$) was associated with a good average accuracy of $200\,000 \text{ m}^3$ (i.e., 7.4 % of the average volume of Lake “la Bure”) of the results, thereby confirming the applicability of this method.

In the second method (Sect. 4.2.), altimetry-based (from ENVISAT RA-2) water levels were similarly combined with ground measurements to estimate the water volumes stored in the lake. This method produced more accurate estimates of the water volumes than the previous method with an average accuracy of $140\,000 \text{ m}^3$ (i.e., 5.2 % of the mean lake volume) and a coefficient of determination of 0.97. The major drawback of

Title Page

Abstract

Introduction

Conclusions

References

Tables

Figures



Back

Close

Full Screen / Esc

Printer-friendly Version

Interactive Discussion



this approach was the low temporal resolution (below one month) of the satellite data. These two methods cannot be generalised because they require in situ data.

Finally, in the third method (Sect. 4.3.), almost-synchronous satellite estimates of water surfaces and levels were used to estimate the variations in the water volume.

5 This approach did not require any in situ measurements and produced promising results ($R^2 = 0.98$), which were better than those obtained using the first two approaches. However, the third method is currently limited by the poor availability of quasi-synchronous remotely sensed observations. In addition, the third method can only be used to calculate changes in the volume and cannot be used to estimate the
10 volume itself. This latter drawback could be overcome by using lake bathymetry.

These results can be used to monitor and manage water resources, especially for agricultural purposes and even for small lakes and reservoirs. A higher spatial resolution and temporal repetitiveness allowing higher quasi-synchronous acquisitions could be achieved by using additional data from current and future satellite missions. Future
15 launches of Sentinel-1, 2, and 3 will provide access to multispectral and SAR HR images combined with a dense temporal sampling (Le Roy et al., 2007; Berger et al., 2012). For radar altimetry, higher accuracy can be expected from the Saral-AltiKa mission over small water bodies because the footprint of the Ka band is smaller than that of the Ku band from current missions. The development of SAR-altimeter (Cryosat-
20 2, Sentinel-3, Jason CS) and SAR-interferometry (SWOT) techniques for altimetry will densify the spatial coverage of radar altimetry over land and ocean, offering high spatial and temporal resolution (ESA Communications, 2012a; ESA Communications 2012b).

Acknowledgements. The authors would like to thank CSA (the Canadian Space Agency), DLR (the German Space Agency) and ESA (the European Space Agency) for providing the Envisat, Terrasar-X, and Radarsat-2 images used in this paper (Projects CSA-SOAR6828, ESA-FRBF1813, and DLR-HYD0611, F. Baup). The authors would also like to thank the Centre de
25 Topographie des Océans et de l'Hydrosphère (CTOH) at Laboratoire d'Etudes en Géophysique et Océanographie Spatiales (LEGOS) for providing the ENVISAT RA-2 GDR dataset. The authors also thank the CNES (Centre National d'Etudes Spatiales) for funding and the CS Company for treating the Formosat-2 images. The authors thank the SIAH group for providing all of
30

[Title Page](#)

[Abstract](#)

[Introduction](#)

[Conclusions](#)

[References](#)

[Tables](#)

[Figures](#)



[Back](#)

[Close](#)

[Full Screen / Esc](#)

[Printer-friendly Version](#)

[Interactive Discussion](#)



the necessary information and the lake management measurements. The authors would also like to thank Sophie Flanquart for her help with the image processing.

References

- Abdul Hakeem, A. and Raju, P. V.: Use of high-resolution satellite data for the structural and agricultural inventory of tank irrigation systems, *Int. J. Remote Sens.*, 30, 3613–3623, 2009.
- 5 Alsdorf, D. E., Rodriguez, E., and Lettenmaier, D. P.: Measuring surface water from space, *Rev. Geophys.*, 45, RG2002, doi:10.1029/2006RG000197, 2007.
- Baup, F., Fieuzal, R., Marais-Sicre, C., Dejoux, J. F., le Dantec, V., Mordelet, P., Claverie, M., Hagolle, O., Lopes, A., Keravec, P., Ceschia, E., Mialon, A., and Kidd, R.: MCM'10: an experiment for satellite multi-sensors crop monitoring from high to low resolution observations, *Geoscience and Remote Sensing Symposium, IEEE International*, 4849–4852, 2011.
- 10 Berger, M., Moreno, J., Johannessen, J. A., Levelt, P. F., and Hanssen, R. F.: ESA's sentinel missions in support of Earth system science, *Remote Sens. Environ.*, 120, 84–90, 2012.
- Birkett, C. M.: The contribution of TOPEX/POSEIDON to the global monitoring of climatically sensitive lakes, *J. Geophys. Res.*, 100, 25179–25204, 1995.
- 15 Birkett, C. M.: Contribution of the TOPEX NASA radar altimeter to the global monitoring of large rivers and wetlands, *Water Resour. Res.*, 34, 1223–1239, 1998.
- Birkett, C. M., Mertes, L. A. K., Dunne, T., Costa, M. H., and Jasinski, M. J.: Surface water dynamics in the Amazon basin: application of satellite radar altimetry, *J. Geophys. Res.*, 107, 8059–8080, 2002.
- 20 Breit, H., Fritz, T., Bals, U., Lachaise, M., Niedermeier, A., and Vonavka, M.: TerraSAR-X SAR processing and products, *IEEE T. Geoscience Remote*, 48, 727–740, 2010.
- Brown, G. S.: The average impulse response of a rough surface and its applications, *Transactions on Antennas and Propagation*, 25, 67–74, 1977.
- 25 Cazenave, A., Bonnefond, P., and Do Minh, K.: Caspian sea level from Topex/Poseidon altimetry: level now falling, *Geophys. Res. Lett.*, 25, 155–158, 1997.
- Chern, J. S., Ling, J., and Weng, S. L.: Taiwan's second remote sensing satellite, *Acta Astronaut.*, 63, 1305–1311, 2008.
- 30 Crétaux, J. F. and Birkett, C.: Lake studies from satellite radar altimetry, *Comptes Rendus Geoscience*, 338, 1098–1112, 2006.

[Title Page](#)

[Abstract](#)

[Introduction](#)

[Conclusions](#)

[References](#)

[Tables](#)

[Figures](#)

[I ◀](#)

[▶ I](#)

[◀](#)

[▶](#)

[Back](#)

[Close](#)

[Full Screen / Esc](#)

[Printer-friendly Version](#)

[Interactive Discussion](#)



[Title Page](#)[Abstract](#)[Introduction](#)[Conclusions](#)[References](#)[Tables](#)[Figures](#)[Back](#)[Close](#)[Full Screen / Esc](#)[Printer-friendly Version](#)[Interactive Discussion](#)

- Crétaux, J. F., Jelinski, W., Calmant, S., Kouraev, A., Vuglinski, V., Bergé Nguyen, M., Gennero, M. C., Nino, F., Del Rio, R. A., Cazenave, A., and Maisongrande, P.: SOLS: a lake database to monitor in the Near Real Time water level and storage variations from remote sensing data, *Adv. Space Res.*, 47, 1497–1507, doi:10.1016/j.asr.2011.01.004, 2011.
- 5 Dejoux, J. F., Dedieu, G., Hagolle, O., Ducrot, D., Menaut, J. C., Ceschia, E., Baup, F., Demarez, V., Marais-Sicre, C., Kadiri, M., and Gascoïn, S.: Kalideos OSR MiPy: un observatoire pour la recherche et la démonstration des applications de la télédétection à la gestion des territoires, *Revue Française de Photogrammétrie et de Télédétection*, 197, 17–30, 2012.
- Ding, X. and Li, X.: Monitoring of the water-area variations of Lake Dongting in China with ENVISAT ASAR images, *Int. J. Appl. Earth Obs.*, 13, 894–901, 2011.
- 10 Duan, Z. and Bastiaanssen, W. G. M.: Estimating water volume variations in lakes and reservoirs from four operational satellite altimetry databases and satellite imagery data, *Remote Sens. Environ.*, 134, 403–416, doi:10.1016/j.rse.2013.03.010, 2013.
- ENVI: Users Guide, version 4.1, available at: http://aviris.gl.fcen.uba.ar/Curso_SR/biblio_sr/ENVI_userguid.pdf, September 2004.
- 15 ESA: ENVISAT RA2/MWR Product handbook, RA2/MWR products user guide, 2002.
- ESA Communications: Sentinel-2: ESA's Optical High-Resolution Mission for GMES Operational Services, ESA SP-1322/2, available at: https://earth.esa.int/web/guest/document-library/-/asset_publisher/2Xho/content/sentinel-2-esa-s-optical-high-resolution-mission-for-gmes-operational-services, 2012a.
- 20 ESA Communications: Sentinel-3: ESA's Global Land and Ocean Mission for GMES Operational Services, ESA SP-1322/3, available at: https://earth.esa.int/web/guest/document-library/-/asset_publisher/2Xho/content/sentinel-3-esa-s-global-land-and-ocean-mission-for-gmes-operational-services, 2012b.
- 25 Fieuzal, R., Baup, F., and Marais-Sicre, C.: Sensitivity of TERRASAR-X, RADARSAT-2 and ALOS satellite radar data to crop variables, *Geoscience and Remote Sensing Symposium, IEEE International*, 3740–3743, 2012.
- Fieuzal, R., Baup, F., Marais-Sicre, C.: Monitoring wheat and rapeseed by using synchronous optical and radar satellite data – from temporal signatures to crop parameters estimation, *Advanced in Remote Sensing*, 2, 162–180, doi:10.4236/ars.2013.22020, 2013.
- 30 Frappart, F., Seyler, F., Martinez, J.-M., Leon, J. G., and Cazenave, A.: Floodplain water storage in the Negro River basin estimated from microwave remote sensing of inundation area and water levels, *Remote Sens. Environ.*, 99, 387–399, 2005.

[Title Page](#)[Abstract](#)[Introduction](#)[Conclusions](#)[References](#)[Tables](#)[Figures](#)[Back](#)[Close](#)[Full Screen / Esc](#)[Printer-friendly Version](#)[Interactive Discussion](#)

Frappart, F., Calmant, S., Cauhopé, M., Seyler, F., and Cazenave, A.: Preliminary results of EN-VISAT RA-2-derived water levels validation over the Amazon basin, *Remote Sens. Environ.*, 100, 252–264, doi:10.1016/j.rse.2005.10.027, 2006a.

Frappart, F., Do Minh, K., L'Hermitte, J., Cazenave, A., Ramillien, G., Le Toan, T., and Mognard-Campbell, N.: Water volume change in the lower Mekong from satellite altimetry and imagery data, *Geophys. J. Int.*, 167, 570–584, doi:10.1111/j.1365-246X.2006.03184.x, 2006b.

Frappart, F., Papa, F., Famiglietti, J. S., Prigent, C., Rossow, W. B., and Seyler, F.: Interannual variations of river water storage from a multiple satellite approach: a case study for the Rio Negro River basin, *J. Geophys. Res.*, 113, D21104, doi:10.1029/2007JD009438, 2008.

Frappart, F., Papa, F., Santos da Silva, J., Ramillien, G., Prigent, C., Seyler, F., and Calmant, S.: Surface freshwater storage and dynamics in the Amazon basin during the 2005 exceptional drought, *Environment Research Letter*, 7, 044010, doi:10.1088/1748-9326/7/4/044010, 2012.

Fritz, T., Eineder, M., Mittermayer, J., Schättler, B., Balzer, W., Buckreuz, S., and Werninghaus, R.: TerraSAR-X ground segment basic product specification document, Cluster Applied Remote Sensing, TX-GS-DD-3302, 108 pp., 2008.

Hagolle, O., Huc, M., Pascual, D. V., and Dedieu, G.: A multi-temporal method for cloud detection, applied to FORMOSAT-2, VENUS, LANDSAT and SENTINEL-2 images, *Remote Sens. Environ.*, 114, 1747–1755, 2010.

Haibo, Y., Zongmin, W., Hongling, Z., and Yu, G.: Water body extraction methods study based on RS and GIS, *Procedia Environmental Sciences*, 10, 2619–2624, 2011.

Hall, A. C., Schumann, G. J. P., Bamber, J. L., and Bates, P. D.: Tracking water level changes of the Amazon Basin with space-borne remote sensing and integration with large scale hydrodynamic modelling: a review, *Phys. Chem. Earth*, 36, 223–231, 2011.

Harding, R., Best, M., Blyth, E., Hagemann, S., Kabat, P., Tallaksen, L. M., Warnars, T., Wiberg, D., Weedon, G. P., van Lanen, H., Ludwig, F., and Haddeland, I.: WATCH: Current Knowledge of the Terrestrial Global Water Cycle, *J. Hydrometeor*, 12, 1149–1156, doi:10.1175/JHM-D-11-024.1, 2011.

Jorgensen, S. E., Loffer, H., Rast, W., and Straskraba, M.: The use of mathematical modelling in lake and reservoir management, in: *Developments in Water Science*, Elsevier, 54, 243–314, 2005.

Kharbouche, S. and Clavet, D.: A tool for semi-automated extraction of waterbody feature in SAR imagery, *Remote Sensing Letters*, 4, 381–390, 2013.

[Title Page](#)[Abstract](#)[Introduction](#)[Conclusions](#)[References](#)[Tables](#)[Figures](#)[◀](#)[▶](#)[◀](#)[▶](#)[Back](#)[Close](#)[Full Screen / Esc](#)[Printer-friendly Version](#)[Interactive Discussion](#)

Klein, I., Dietz, A. J., Gessner, U., Galayeva, A., Myrzakhmetov, A., and Kuenzer, C.: Evaluation of seasonal water body extents in Central Asia over the past 27 years derived from medium-resolution remote sensing data, *Int. J. Appl. Earth Obs.*, 26, 335–349, 2014.

Kuemmerle, T., Erb, K., Meyfroidt, P., Müller, D., Verburg, P. H., Estel, S., and Reenberg, A.: Challenges and opportunities in mapping land use intensity globally, *Curr. Opin. Environ. Sustain.*, 5, 484–493, doi:10.1016/j.cosust.2013.06.002, 2013.

Lavalle, M. and Wright, T.: Absolute radiometric and polarimetric calibration of ALOS PALSAR products, available at: http://earth.eo.esa.int/pcs/alos/palsar/articles/Calibration_palsar_products_v13.pdf, 2009.

Laxon, S.: Sea ice altimeter processing scheme at the EODC, *Int. J. Remote Sens.*, 15, 915–924, 1994.

Le Roy, Y., Deschaux-Beaume, M., Mavrocordatos, C., Aguirre, M., and Heliere, F.: SRAL SAR radar altimeter for Sentinel-3 mission, *Geoscience and Remote Sensing Symposium, IEEE International*, 219–222, 2007.

Legrésy, B. and Rémy, F.: Surface characteristics of the Antarctic ice sheet and altimetric observations. *J. Glaciol.*, 43, 197–206, 1997.

Lillesand, T., Kiefer, R., and Chipman, J. W.: *Remote Sensing and Image Interpretation*, Sixth Edition, John Wiley and Sons, Inc., New York, 768 pp., 2008.

Liu, C. C.: Processing of FORMOSAT-2 daily revisit imagery for site surveillance, *IEEE T. Geosci. Remote*, 44, 3206–3214, 2006.

Morena, L. C., James, K. V., and Beck, J.: An introduction to the RADARSAT-2 mission, *Can. J. Remote Sens.*, 30, 221–234, 2004.

NEST (Next ESA SAR Toolbox): User manual-5.0, available at: <http://nest.array.ca/web/nest/documentation> (last access: 18 December 2013), 2013.

Richards, J. A.: *Remote Sensing Digital Image Analysis*, Springer, Berlin, 240 pp., 1999.

Ricko, M., Birkett, C., Carton, J. A., and Crétaux J- F.: Intercomparison and validation of continental water level products derived from satellite radar altimetry, *J. Appl. Remote Sens.*, 6, 061710, doi:10.1117/1.JRS.6.061710, 2012.

OECD: *Water Quality and Agriculture: Meeting the Policy Challenge*, OECD Studies on Water, OECD Publishing, doi:10.1787/9789264168060-en, IWA Publishing, London, UK, 2012.

Sand, A. and De Boissezon, H.: Reference remote sensing data bases: temporal series of calibrated and ortho-rectified satellite images for scientific use, *2nd International Symposium on Recent Advances in Quantitative Remote Sensing*, Torrent, Spain, 2006.

[Title Page](#)[Abstract](#)[Introduction](#)[Conclusions](#)[References](#)[Tables](#)[Figures](#)[◀](#)[▶](#)[◀](#)[▶](#)[Back](#)[Close](#)[Full Screen / Esc](#)[Printer-friendly Version](#)[Interactive Discussion](#)

Santos da Silva, J., Calmant, S., Seyler, F., Rotunno Filho, O. C., Cochonneau, G., and Mansur, W. J.: Water levels in the Amazon basin derived from the ERS 2 and ENVISAT radar altimetry missions, *Remote Sens. Environ.*, 114, 2160–2181, doi:10.1016/j.rse.2010.04.020, 2010.

5 Santos da Silva, J., Seyler, F., Calmant, S., Corrêa Rotuno Filho, O., Roux, E., Magalhaes, A. A., and Guyot, J.-L.: Water level dynamics of Amazon wetlands at the watershed scale by satellite altimetry, *Int. J. Remote Sens.*, 33, 200–206, 2012.

Skriver, H., Svendsen, M. T., and Thomsen, A. G.: Multitemporal C-and L-band polarimetric signatures of crops, *IEEE T. Geosci. Remote*, 37, 2413–2429, 1999.

10 Strozzi, T., Wiesmann, A., Käab, A., Joshi, S., and Mool, P.: Glacial lake mapping with very high resolution satellite SAR data, *Nat. Hazards Earth Syst. Sci.*, 12, 2487–2498, doi:10.5194/nhess-12-2487-2012, 2012.

White, D. C. and Lewis, M.: A new approach to monitoring spatial distribution and dynamics of wetlands and associated flows of Australian Great Artesian Basin springs using QuickBird satellite imagery, *J. Hydrol.*, 408, 140–152, 2011.

15 Wingham, D. J., Rapley, C. G., and Griffiths, H.: New techniques in satellite altimeter tracking systems, in: *Proceedings of IGARSS'86 Symposium*, Ref. ESA SP-254, 1339–1344, 1986.

Yesou, H., Allenbach, B., Andreoli, R., Battiston, S., Bestault, C., Clandillon, S., and de Fraipont, P.: Synergy of High SAR and optical data for flood monitoring; the 2005–2006 Central European floods gained experience, *Proceeding Envisat Symposium*, 22–25 April 2007, *Proceedings ESA ENVISAT Montreux Symposium*, Switzerland, 2007.

20 Zelli, C.: ENVISAT RA-2 advanced radar altimeter: instrument design and pre-launch performance assessment review, *Acta Astronaut.*, 44, 323–333, 1999.

25 Zhou, H., Jiang, H., Zhou, G., Song, X., Yu, S., Chang, J., and Jiang, B.: Monitoring the change of urban wetland using high spatial resolution remote sensing data, *Int. J. Remote Sens.*, 31, 1717–1731, 2010.

HESSD

10, 15731–15770, 2013

Volume of small lakes

F. Baup et al.

Title Page

Abstract

Introduction

Conclusions

References

Tables

Figures

◀

▶

◀

▶

Back

Close

Full Screen / Esc

Printer-friendly Version

Interactive Discussion



Table 1. Characteristics of the electromagnetic waves of satellite sensors (in optical and microwave frequencies).

Satellite	Frequency/wavelength	Mode	Polarisation states	Range of incidence angle
Radarsat-2	C-band ($f = 5.405$ GHz)	FQ	HH, VV, VH, HV	23° to 41°
Terrasar-X	X-band ($f = 9.65$ GHz)	SM/SL	HH	27° to 53°
Formosat-2	λ : 0.44–0.90 μm	Multi-spectral	–	$\pm 45^\circ$

HESSD

10, 15731–15770, 2013

Volume of small lakes

F. Baup et al.

[Title Page](#)[Abstract](#)[Introduction](#)[Conclusions](#)[References](#)[Tables](#)[Figures](#)[Back](#)[Close](#)[Full Screen / Esc](#)[Printer-friendly Version](#)[Interactive Discussion](#)**Table 2.** Summary of ground data used.

Ground data	Dates	Sampling frequency
Lake calibration function (abacus)	In 1987	–
Bathymetric draw	In 2010	–
Water level	since 2003	Weekly
Rainfall	since 2006	Daily

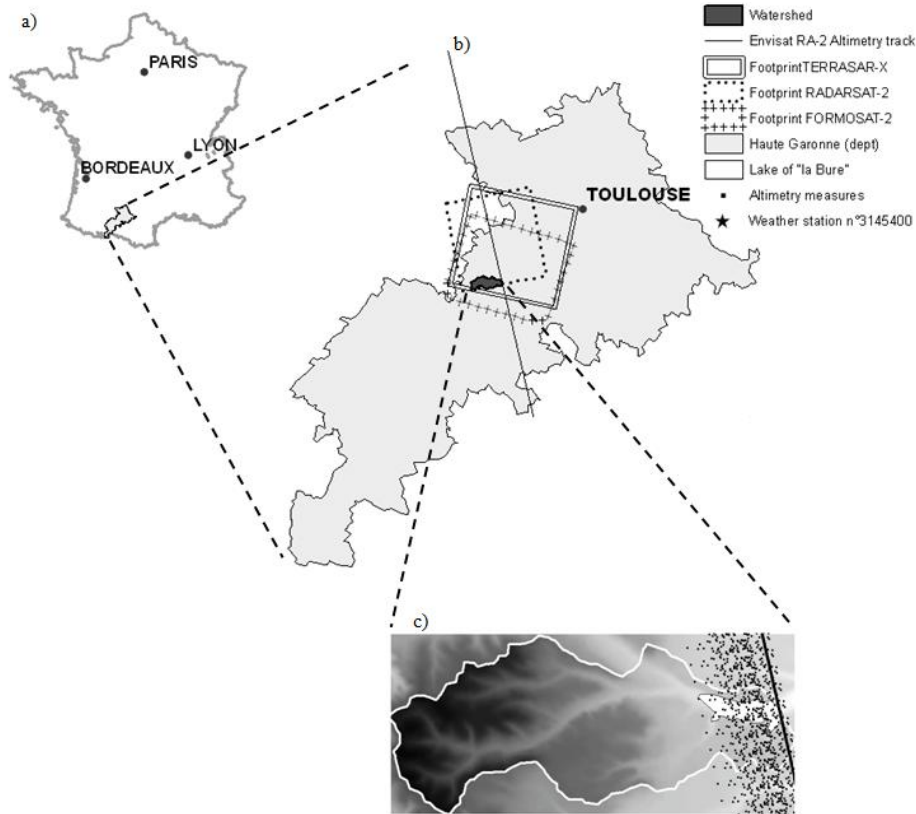


Fig. 1. Lake "la Bure" is located in the south-west of France 40 km south-west of Toulouse (a), within the footprint of TERRASAR-X (white empty rectangle), RADARSAT-2 (dotted empty rectangle), and FORMOSAT-2 (empty rectangle of crosses) and under ENVISAT RA-2 altimetry track 773 (b); the black dots represent 20 Hz altimetry measurements over Lake "la Bure" (c).

HESSD

10, 15731–15770, 2013

Volume of small lakes

F. Baup et al.

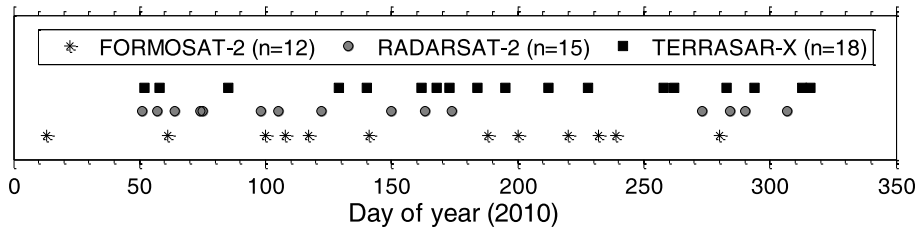


Fig. 2. Timeline for acquisition of high spatial resolution satellite images in 2010.

Title Page

Abstract Introduction

Conclusions References

Tables Figures

◀ ▶

◀ ▶

Back Close

Full Screen / Esc

Printer-friendly Version

Interactive Discussion



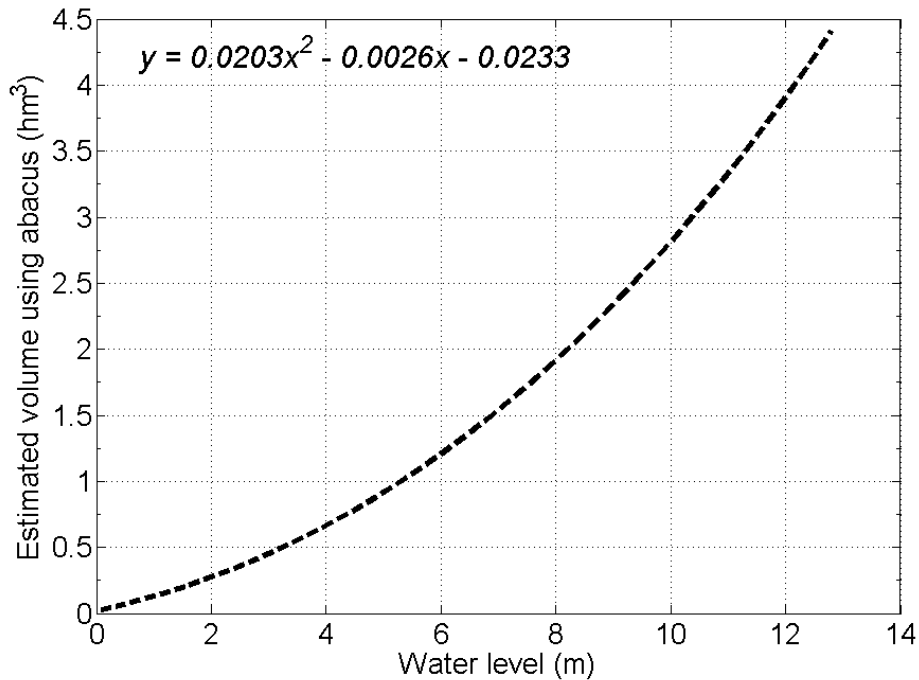


Fig. 3. Relationship between in situ water levels and the volumes of lake “la Bure” established in 1987.

HESSD

10, 15731–15770, 2013

Volume of small lakes

F. Baup et al.

[Title Page](#)
[Abstract](#) [Introduction](#)
[Conclusions](#) [References](#)
[Tables](#) [Figures](#)
[◀](#) [▶](#)
[◀](#) [▶](#)
[Back](#) [Close](#)
[Full Screen / Esc](#)
[Printer-friendly Version](#)
[Interactive Discussion](#)



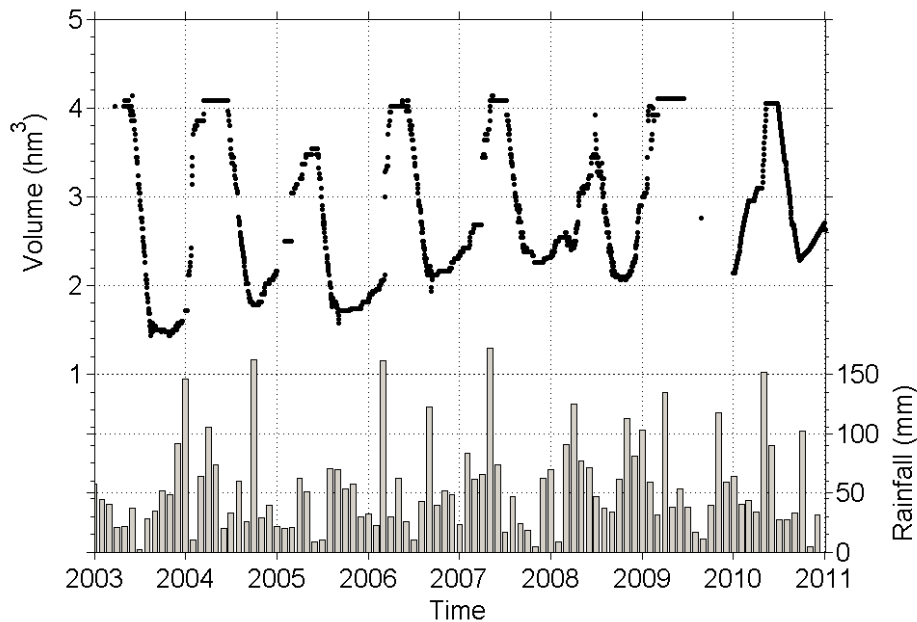


Fig. 4. Temporal variations of the local rainfall and measured water volume of Lake “la Bure” (black dots) from 2003 to 2011.

[Title Page](#)[Abstract](#)[Introduction](#)[Conclusions](#)[References](#)[Tables](#)[Figures](#)[Back](#)[Close](#)[Full Screen / Esc](#)[Printer-friendly Version](#)[Interactive Discussion](#)

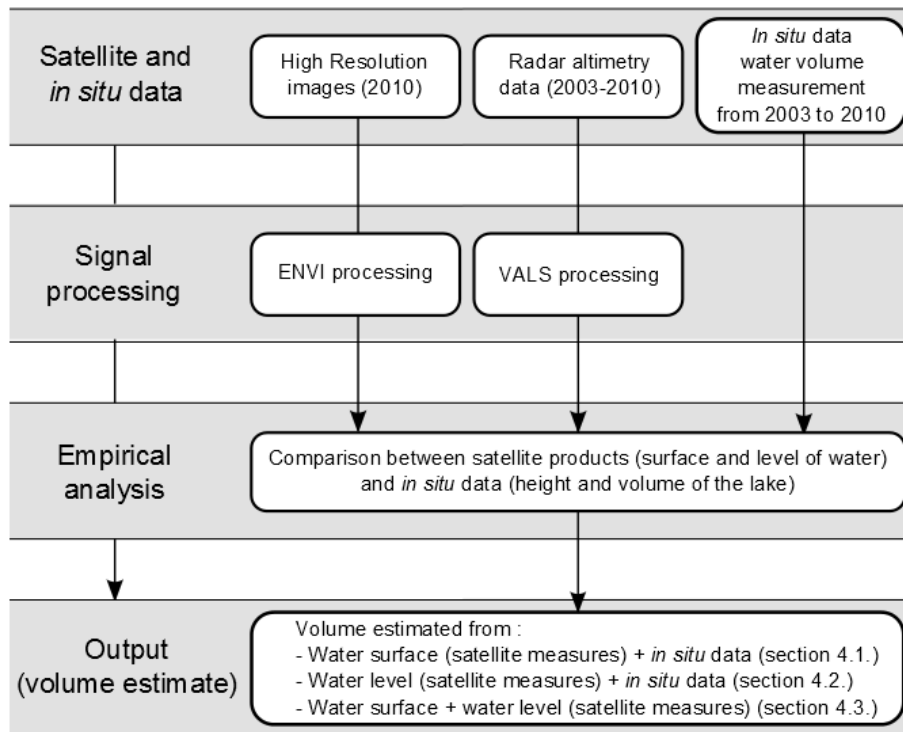


Fig. 5. Flowchart showing the processing steps used to estimate the volume of Lake “la Bure” using high-resolution images (HR), radar altimetry (RA-2), and ground data for each of the three methods.

[Title Page](#)
[Abstract](#)
[Introduction](#)
[Conclusions](#)
[References](#)
[Tables](#)
[Figures](#)
[⏪](#)
[⏩](#)
[◀](#)
[▶](#)
[Back](#)
[Close](#)
[Full Screen / Esc](#)
[Printer-friendly Version](#)
[Interactive Discussion](#)

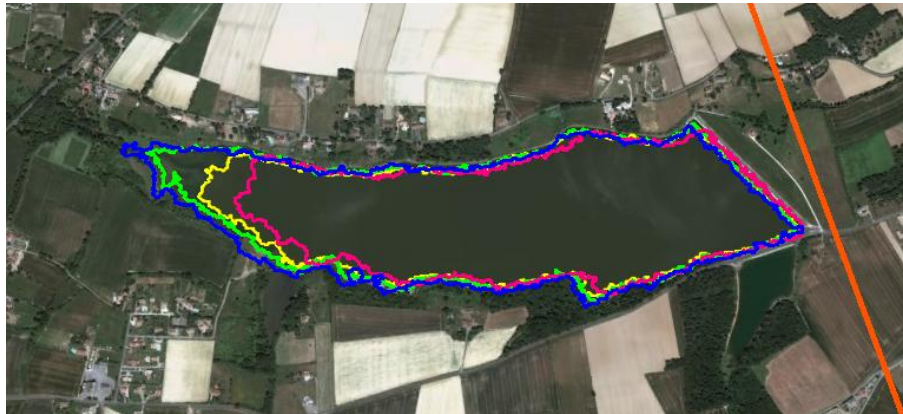



Fig. 6. Examples of temporal evolution of the lake shorelines resulting of the supervised classification of Radarsat-2 image: the green, blue, yellow, and pink lines represent the lake shoreline on 31 May, 23 June, 11 November, and 30 September 2010, respectively; the orange line to the east of the lake represents the theoretical groundtrack of the Envisat altimeter.

[Title Page](#)[Abstract](#)[Introduction](#)[Conclusions](#)[References](#)[Tables](#)[Figures](#)[⏪](#)[⏩](#)[◀](#)[▶](#)[Back](#)[Close](#)[Full Screen / Esc](#)[Printer-friendly Version](#)[Interactive Discussion](#)

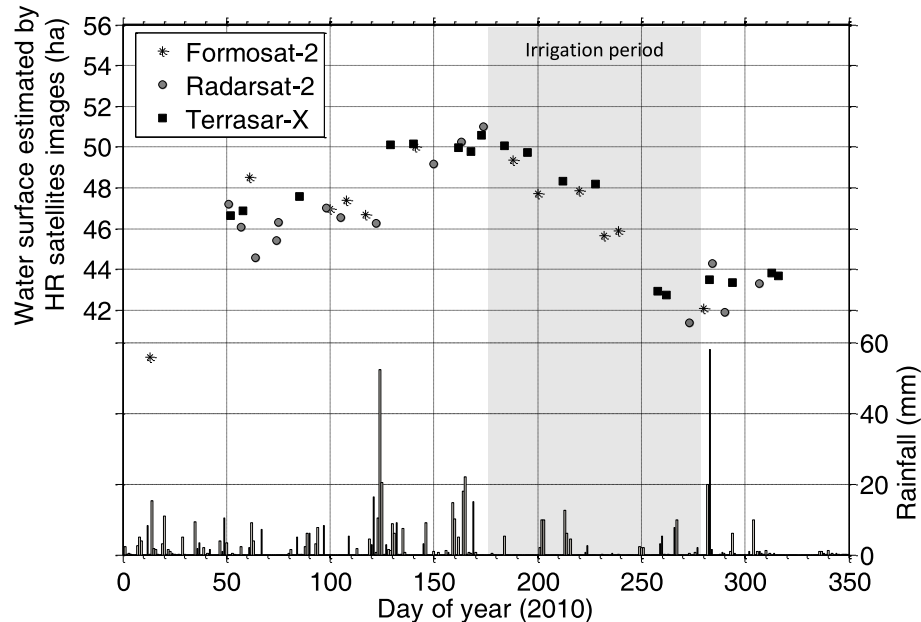


Fig. 7. Temporal evolution of water surface of lake “la Bure”, as estimated by HR satellite images in 2010 (TerraSAR-X data are shown as black squares, Radarsat-2 as gray circle, Formosat-2 as black stars and irrigation period as gray rectangle).

[Title Page](#)
[Abstract](#)
[Introduction](#)
[Conclusions](#)
[References](#)
[Tables](#)
[Figures](#)
[◀](#)
[▶](#)
[◀](#)
[▶](#)
[Back](#)
[Close](#)
[Full Screen / Esc](#)
[Printer-friendly Version](#)
[Interactive Discussion](#)

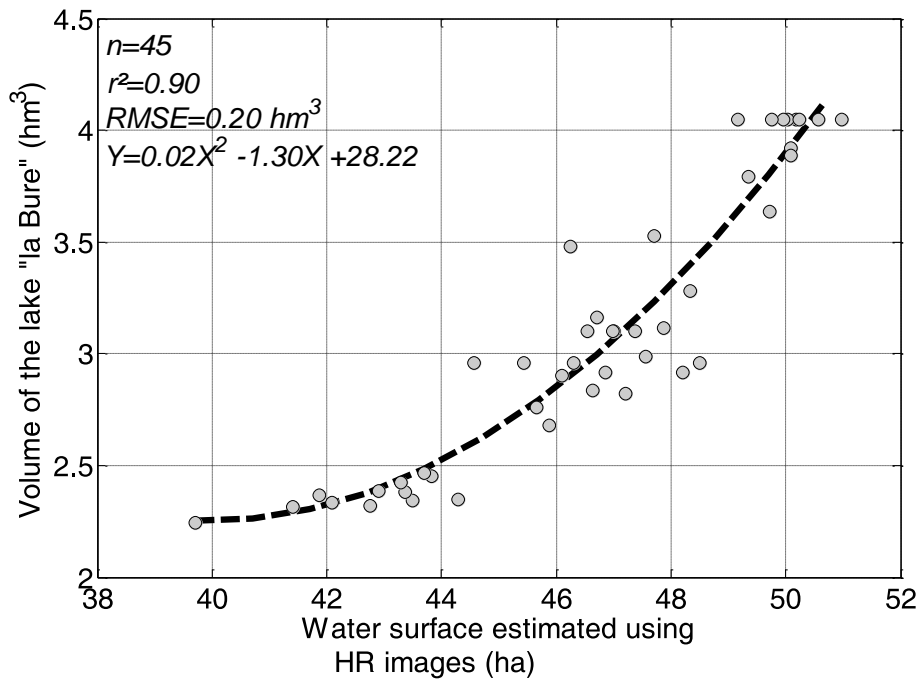



Fig. 8. Empirical relationship between surface products (from HR satellite images) and volume data (SIAH) that were recorded on the same day.

Title Page

Abstract	Introduction
Conclusions	References
Tables	Figures

⏪
⏩

◀
▶

Back	Close
------	-------

Full Screen / Esc

Printer-friendly Version

Interactive Discussion



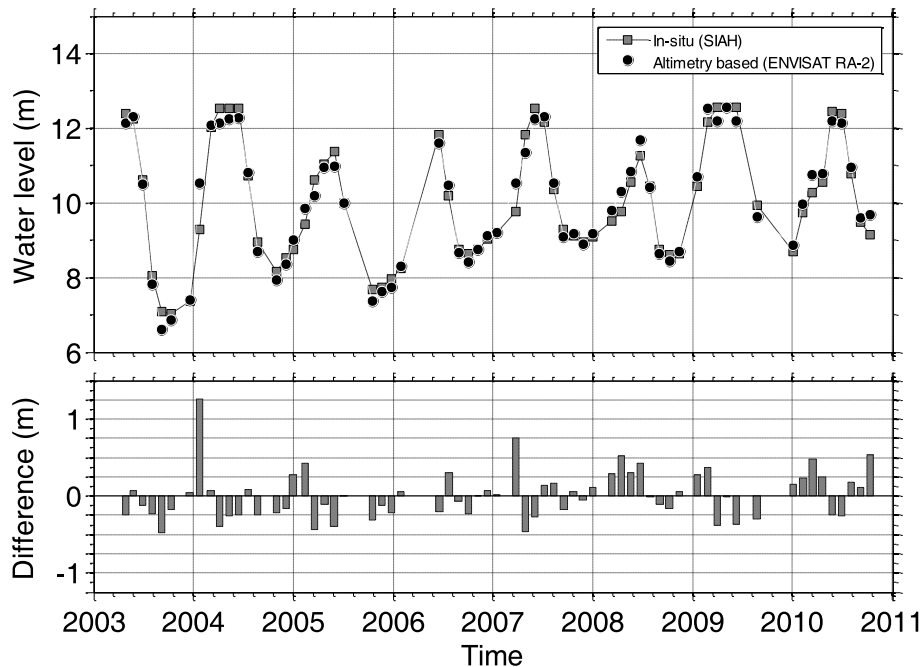


Fig. 9. Comparison of satellite-estimated (RA-2) and ground-measured (SIAH) time series of the water level of lake “la Bure” from 2003 to 2010.

[Title Page](#)[Abstract](#)[Introduction](#)[Conclusions](#)[References](#)[Tables](#)[Figures](#)[◀](#)[▶](#)[◀](#)[▶](#)[Back](#)[Close](#)[Full Screen / Esc](#)[Printer-friendly Version](#)[Interactive Discussion](#)

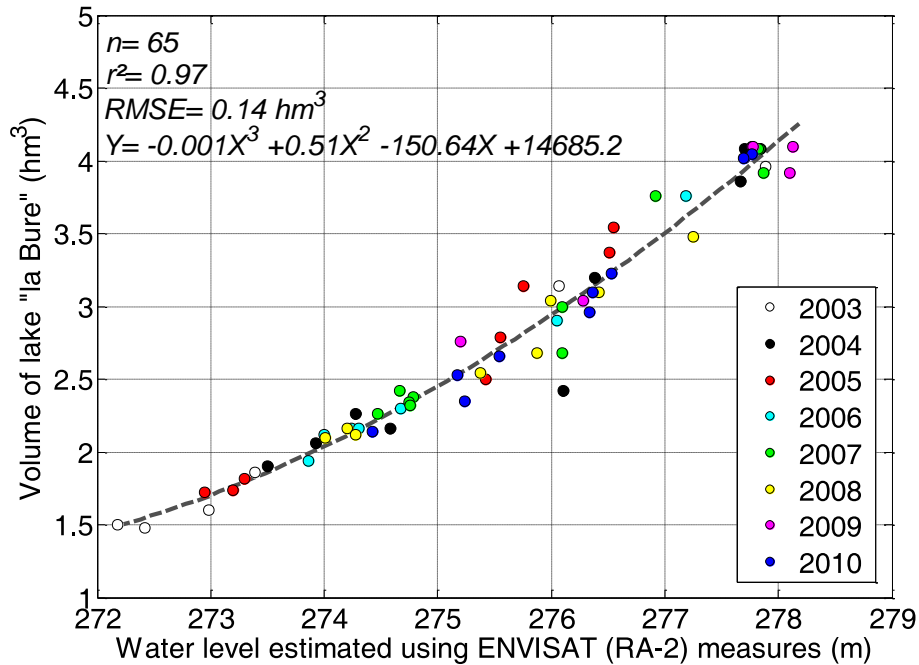


Fig. 10. Empirical relationship between the satellite water level (RA-2) and the measured (SIAH) water volume of lake "la Bure" from 2003 to 2010. Each year is colour-separated.

Title Page

Abstract Introduction

Conclusions References

Tables Figures

◀ ▶

◀ ▶

Back Close

Full Screen / Esc

Printer-friendly Version

Interactive Discussion



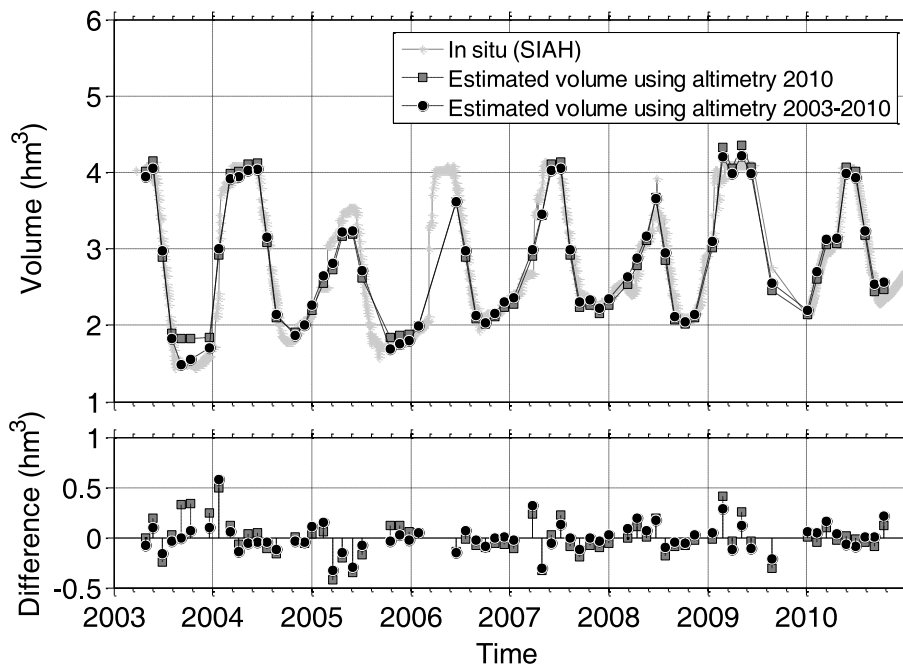


Fig. 11. Comparisons of temporal evolution of water volume of the lake of interest, estimated by using two calibration functions: annual (2010) and pluri-annual (2003–2010). The differences between these results and the ground measurements are also shown.

[Title Page](#)[Abstract](#)[Introduction](#)[Conclusions](#)[References](#)[Tables](#)[Figures](#)[◀](#)[▶](#)[◀](#)[▶](#)[Back](#)[Close](#)[Full Screen / Esc](#)[Printer-friendly Version](#)[Interactive Discussion](#)

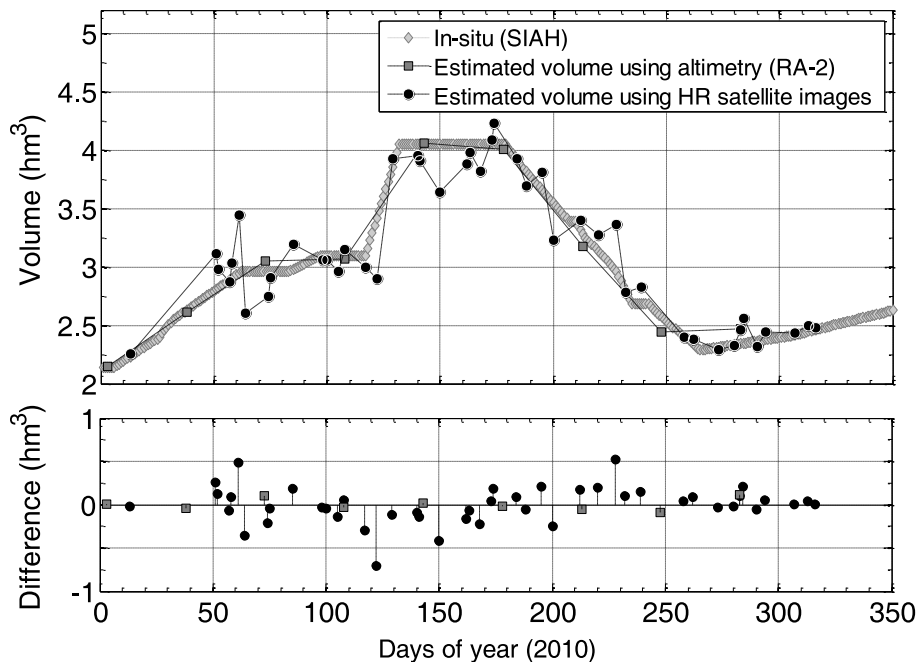


Fig. 12. Comparison between volume estimates from altimeter and image products (water levels and surfaces); grounds measurements are displayed in gray.

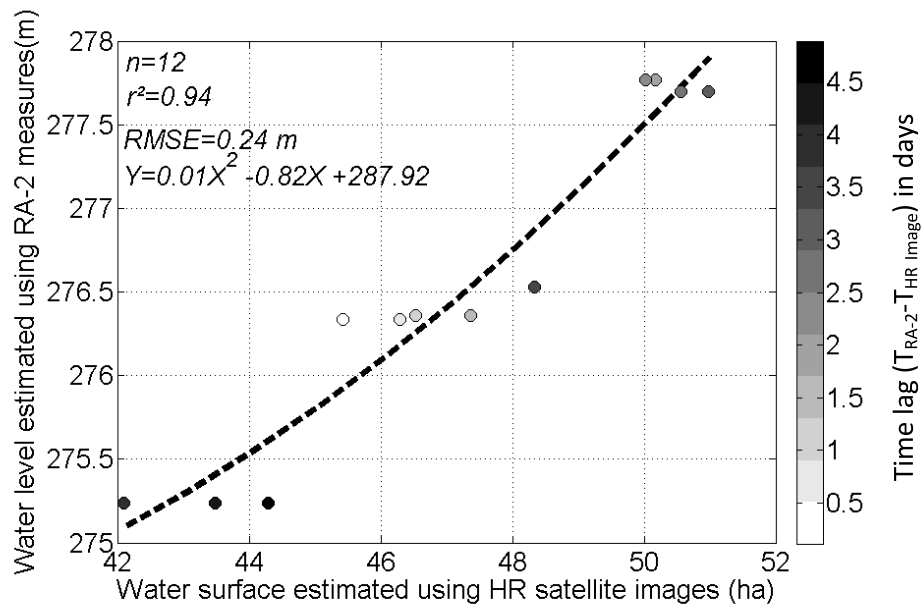


Fig. 13. Relationship between satellite water surface (HR images) and water level products (altimetry) acquired with a time lag of less than 5 days.

[Title Page](#)
[Abstract](#)
[Introduction](#)
[Conclusions](#)
[References](#)
[Tables](#)
[Figures](#)
[⏪](#)
[⏩](#)
[◀](#)
[▶](#)
[Back](#)
[Close](#)
[Full Screen / Esc](#)
[Printer-friendly Version](#)
[Interactive Discussion](#)

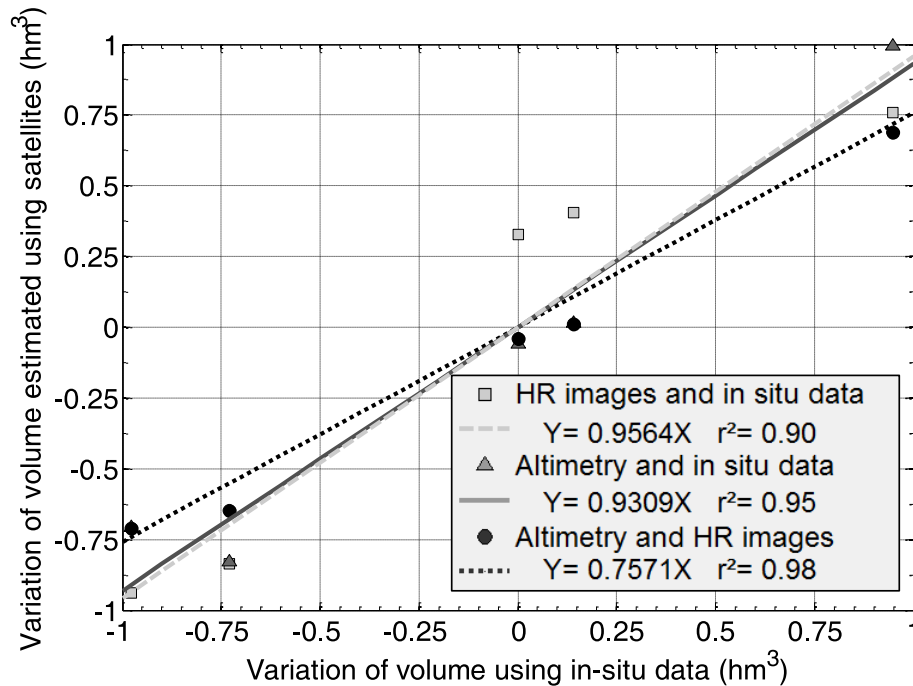



Fig. 14. Comparison between the variation in the water volume estimated by satellite data and ground-measured (SIAH) data in 2010.

[Title Page](#)
[Abstract](#)
[Introduction](#)
[Conclusions](#)
[References](#)
[Tables](#)
[Figures](#)
[◀](#)
[▶](#)
[◀](#)
[▶](#)
[Back](#)
[Close](#)
[Full Screen / Esc](#)
[Printer-friendly Version](#)
[Interactive Discussion](#)
